Continuum level density of a coupled-channel system in the complex scaling method

Ryusuke Suzuki, András T. Kruppa, Bertrand G. Giraud, Kiyoshi Katō

Continuum Level Density of a Coupled-Channel System in the Complex Scaling Method

Ryusuke Suzuki,[1,*] András T. Kruppa,[2,**] Bertrand G. Giraud[3,***] and Kiyoshi Katō [1,†]

[1] *Division of Physics, Graduate School of Science, Hokkaido University, Sapporo 060-0810, Japan*
[2] *Institute of Nuclear Research, Bem tér 18/c, 4026 Debrecen, Hungary*
[3] *Institut de Physique Théorique, DSM, CE Saclay, F-91191 Gif/Yvette, France*

We study the continuum level density (CLD) in the formalism of the complex scaling method (CSM) for coupled-channel systems. We apply the formalism to the $^4\text{He} = [^3\text{H}+p] + [^3\text{He}+n]$ coupled-channel cluster model where there are resonances at low energy. Numerical calculations of the CLD in the CSM with a finite number of L^2 basis functions are consistent with the exact result calculated from the S-matrix by solving coupled-channel equations. We also study channel densities. In this framework, the extended completeness relation (ECR) plays an important role.

§1. Introduction

The continuum level density (CLD),[1]–[3] $\Delta(E)$, plays an important role in the description of scattering phenomena and structures of nuclei since the CLD connects the scattering S-matrix[4]–[6]

$$\Delta(E) = \frac{1}{2\pi}\text{Im}\frac{d}{dE}\ln \det S(E) \tag{1·1}$$

with the Green functions

$$\Delta(E) = -\frac{1}{\pi}\text{Im}\left[\text{Tr}\left\{G(E+i0) - G_0(E+i0)\right\}\right], \tag{1·2}$$

where the full and free Green functions are given by $G(z) = (z-H)^{-1}$ and $G_0(z) = (z-H_0)^{-1}$, respectively. The notation $G(E+i0)$ $(G_0(E+i0))$ stands for the following limit,

$$\lim_{\epsilon\to+0} G(E + i\epsilon). \qquad (\lim_{\epsilon\to+0} G_0(E + i\epsilon))$$

The CLD of a single particle spectrum has been well investigated[1]–[3],[7),8)] and applied to the cluster model.[9] Recently, we have shown that the combination of the complex scaling method (CSM)[10]–[13] and the basis function method provides a great help for calculating the CLD.[14] In this formalism, the CLD can be obtained

*) E-mail: ryusuke@nucl.sci.hokudai.ac.jp
**) E-mail: atk@atomki.hu
***) E-mail: bertrand.giraud@cea.fr
†) E-mail: kato@nucl.sci.hokudai.ac.jp

from the eigenvalues of the complex-scaled Hamiltonian, $H(\theta)$, and the asymptotic Hamiltonian, $H_0(\theta)$, in which a finite number of L^2 basis functions are used for diagonalization. Usually, the CSM is used to obtain the energies and widths of the resonant states with the L^2 basis functions as well as the energies of the bound states. Simultaneously, an advantage of the complex scaling in calculations of the CLD is a reduction of the cumbersome problem of smoothing[15)–17)] the contribution from the discretized continuum states obtained with the L^2 basis functions.

In our previous paper,[14)] the applicability of the formalism was confirmed in single-channel systems, such as $^5\mathrm{He} = {}^4\mathrm{He} + n$, $^8\mathrm{Be} = \alpha + \alpha$, and we also confirmed that the scattering phase shift is obtained from the eigenvalues of the complex-scaled Hamiltonian. The next question is how we can apply this method to more complex systems, such as coupled-channel systems or three-body systems.

In this paper, we discuss the applicability of the CLD within the CSM to coupled-channel systems and discuss the extended completeness relation (ECR) in the CSM. The ECR was originally discussed in Ref. 18) and the ECR in the CSM has been discussed in Ref. 19). The mathematical proof of the ECR for the coupled-channel problems has been recently given,[20), 21)] and we show here its numerical verification.

In §2, we explain the CLD formalism, and in §3, its application to the coupled-channel cluster model is shown. In §4, we study channel densities, and a summary and conclusions are given in §5.

§2. Continuum level density

2.1. *CLD in coupled-channel systems*

In this section, we explain the CLD in a coupled-channel system. Here, we formulate a treatment of the CLD using the coupled-channel formalism.

Before discussing the coupled-channel problem, we explain the explicit representation of the CLD in single-channel systems. As shown in the right-hand side of Eq. (1·2), the CLD is represented as

$$\Delta(E) = -\frac{1}{\pi}\mathrm{Im}\int d\boldsymbol{r}\left\{\left\langle \boldsymbol{r}\left|\frac{1}{E+i0-H}\right|\boldsymbol{r}\right\rangle - \left\langle \boldsymbol{r}\left|\frac{1}{E+i0-H_0}\right|\boldsymbol{r}\right\rangle\right\}. \quad (2\cdot1)$$

For systems having only bound states the level density is defined in a similar form

$$-\frac{1}{\pi}\mathrm{Im}\int d\boldsymbol{r}\left\langle \boldsymbol{r}\left|\frac{1}{E+i0-H}\right|\boldsymbol{r}\right\rangle \quad (2\cdot2)$$

and a simple calculation gives the expected result, $\sum_B \delta(E - E_B)$, where the bound state energies are denoted by E_B. The CLD in Eq. (2·1) is a generalization of the level density of bound states to include resonant states produced by interactions in the energy region of the continuum.

Next, we study a two-body coupled-channel system of n channels, where each channel $\{\alpha; \ \alpha = 1, \ldots, n\}$ is described by a relative radial wavefunction, $\chi_\alpha(r_\alpha)$, and a channel wavefunction, Φ_α ($\langle\langle\Phi_\alpha|\Phi_\beta\rangle\rangle = \delta_{\alpha,\beta}$), where the double bracket $\langle\langle|\rangle\rangle$ indicates integration for internal degrees of clusters and angular coordinates of relative motion between clusters. Therefore, the total wavefunction of the system is

expressed as

$$|\Psi\rangle = \sum_{\alpha=1}^{n} \chi_\alpha(r_\alpha)|\Phi_\alpha(\hat{\boldsymbol{r}}_\alpha)\rangle\rangle. \tag{2·3}$$

The Hamiltonian H of the coupled-channel system is given as a sum of the asymptotic term H_0 and the short-range interaction V,

$$H = H_0 + V. \tag{2·4}$$

These are

$$H_0 = \sum_{\alpha=1}^{n} (T_\alpha + \epsilon_\alpha)|\Phi_\alpha\rangle\rangle\langle\langle\Phi_\alpha|, \tag{2·5a}$$

$$V = \sum_{\alpha,\beta=1}^{n} V_{\alpha\beta}|\Phi_\alpha\rangle\rangle\langle\langle\Phi_\beta|, \tag{2·5b}$$

where T_α, ϵ_α and $V_{\alpha\beta}$ are the radial kinetic energy, the channel energy corresponding to the threshold of the α channel, and the interaction coupling the α and β channels, respectively. We here assume that $\epsilon_1 \leq \epsilon_2 \leq \cdots \leq \epsilon_n$.

The trace operation in Eq. (2·1) for a single channel case is replaced as $\int d\boldsymbol{r} \rightarrow \sum_{\alpha=1}^{n}\langle\langle\Phi_\alpha(\hat{\boldsymbol{r}}_\alpha)| \int r_\alpha^2 dr_\alpha$ in the coupled-channel system, and we have

$$\Delta(E) = -\frac{1}{\pi}\text{Im}\sum_{\alpha=1}^{n} \int r_\alpha^2 dr_\alpha \,\langle\langle\Phi_\alpha| \left\langle \boldsymbol{r_\alpha} \left| \frac{1}{E + i0 - H} - \frac{1}{E + i0 - H_0} \right| \boldsymbol{r_\alpha} \right\rangle |\Phi_\alpha\rangle\rangle. \tag{2·6}$$

2.2. *CLD in complex scaling method*

In the CSM for coupled-channel systems, the relative coordinate $\boldsymbol{r}_\alpha$ and the conjugate wave number $\boldsymbol{k}_\alpha$ of every channel are commonly transformed as

$$U(\theta) : \boldsymbol{r}_\alpha \rightarrow \boldsymbol{r}_\alpha \exp(i\theta), \qquad \boldsymbol{k}_\alpha \rightarrow \boldsymbol{k}_\alpha \exp(-i\theta), \tag{2·7}$$

where $U(\theta)$ is a scaling operator and θ is a real number called a scaling parameter.

Under this transformation, because of their damping behaviors in the asymptotic region, resonant states and bound states are obtained as discrete solutions of the complex-scaled Schrödinger equation

$$H(\theta)\Psi^\theta = E\Psi^\theta, \tag{2·8}$$

where $H(\theta)$ is the complex-scaled Hamiltonian, $H(\theta) = U(\theta)HU^{-1}(\theta)$. The continuum spectra of the Hamiltonian $H(\theta)$ are distributed on the 2θ-lines originating from the threshold energies of the channels, as shown in Fig. 1.

In Fig. 1, a schematic eigenvalue distribution of coupled-channel systems is illustrated. The 2θ-lines are the rotated branch cuts of the multisheet Riemann surface. In addition to bound states with negative energies, where the energy E is measured from the lowest channel threshold energy assigned as the origin, complex eigenvalues
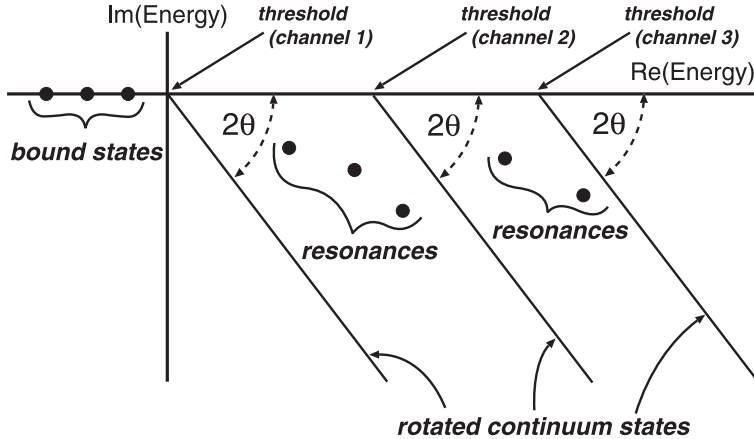
Fig. 1.   Schematic energy eigenvalue distribution of a complex scaled Hamiltonian.

of the resonances are obtained in the wedge region surrounded by the lowest channel 2θ-line and the real axis. The resonant states obtained in the energy strip between two 2θ-lines of the m- and $(m+1)$-channels have the asymptotic property of a closed behavior for the $(m+1, \cdots, n)$ channels while they can have an open behavior for the $(1, \cdots, m)$ channels.

For the solutions of the complex-scaled Schrödinger equation (2·8), we have the extended completeness relation (ECR),[18),19)] which was proven for single- and coupled-channel cases in Refs. 20) and 21), respectively,

$$1 = \sum_{B}^{N_B} |\Psi_{k_B}^{\theta}\rangle\langle\tilde{\Psi}_{k_B}^{\theta}| + \sum_{R}^{N_R^{\theta}} |\Psi_{k_R}^{\theta}\rangle\langle\tilde{\Psi}_{k_R}^{\theta}| + \sum_{\alpha=1}^{n} \int dE_{k_\theta^\alpha} |\Psi_{k_\theta^\alpha}^{\theta}\rangle\langle\tilde{\Psi}_{k_\theta^\alpha}^{\theta}|. \qquad (2\cdot9)$$

The number of bound states $\Psi_{k_B}^{\theta}$ is denoted by N_B, and N_R^{θ} denotes the number of resonant solutions $\Psi_{k_R}^{\theta}$ extracted as isolated eigenstates of $H(\theta)$ for a given scaling parameter θ. The integration in the third term is performed along the rotated branch cuts (the 2θ-lines) of $\alpha = 1 \sim n$ channels. The bra-states with a tilde are biorthogonal to the ket-states.[18)]

Applying the complex scaling defined in Eq. (2·7) and the ECR given in Eq. (2·9) to the CLD in Eq. (2·6), we obtain

$$\Delta(E) = -\frac{1}{\pi}\mathrm{Im}\sum_{\alpha=1}^{n}\int r_\alpha^2 dr_\alpha \langle\langle\Phi_\alpha| \left\langle \boldsymbol{r}_\alpha \left| U(\theta)^{-1}U(\theta)\left(\frac{1}{E+i0-H} - \frac{1}{E+i0-H_0}\right)\right.\right.$$
$$\left.\left. \times U(\theta)^{-1}U(\theta)\right| \boldsymbol{r}_\alpha\right\rangle |\Phi_\alpha\rangle\rangle$$

$$= -\frac{1}{\pi}\mathrm{Im}\sum_{\alpha=1}^{n}\int r_\alpha^2 dr_\alpha \langle\langle\Phi_\alpha| \left\langle \boldsymbol{r}_\alpha^\theta \left| \left(\frac{1}{E-H(\theta)} - \frac{1}{E-H_0(\theta)}\right)\right| \boldsymbol{r}_\alpha^\theta\right\rangle |\Phi_\alpha\rangle\rangle$$

$$= -\frac{1}{\pi}\mathrm{Im}\sum_{\alpha=1}^{n}\int r_\alpha^2 dr_\alpha \langle\langle\Phi_\alpha| \left[\sum_{B}^{N_B} \frac{|\Psi_{k_B}^{\theta}\rangle\langle\tilde{\Psi}_{k_B}^{\theta}|}{E-E_B} + \sum_{R}^{N_R^{\theta}} \frac{|\Psi_{k_R}^{\theta}\rangle\langle\tilde{\Psi}_{k_R}^{\theta}|}{E-E_R}\right.$$

$$+\sum_{\beta=1}^{n}\int dE_{k_\theta^\beta}\frac{|\Psi_{k_\theta^\beta}^\theta\rangle\langle\tilde\Psi_{k_\theta^\beta}^\theta|}{E-E_{k_\theta^\beta}}-\sum_{\beta=1}^{n}\int dE_{k_\theta^\beta,0}\frac{|\Psi_{k_\theta^\beta,0}^\theta\rangle\langle\tilde\Psi_{k_\theta^\beta,0}^\theta|}{E-E_{k_\theta^\beta,0}}\Bigg]|\Phi_\alpha\rangle\rangle,\quad(2\cdot10)$$

where the complex-scaled total wavefunctions Ψ_k^θ and $\tilde\Psi_k^\theta$ are expressed as

$$|\Psi_k^\theta\rangle=\sum_{\beta=1}^{n}\chi_\beta^\theta(k,\ r_\beta)|\Phi_\beta\rangle\rangle\quad\text{and}\quad\langle\tilde\Psi_k^\theta|=\sum_{\beta=1}^{n}\tilde\chi_\beta^{\theta*}(k,\ r_\beta)\langle\langle\Phi_\beta|,\qquad(2\cdot11)$$

respectively. The scalar product of the complex scaled radial wave functions $\chi_\alpha^\theta(k,\ r_\alpha)$ and $\tilde\chi_\alpha^\theta(k,\ r_\alpha)$ is defined as the so-called c-product,[12),22)]

$$\int r_\alpha^2 dr_\alpha\chi_\alpha^\theta(k,\ r_\alpha)\tilde\chi_\alpha^{\theta*}(k,\ r_\alpha)=\int r_\alpha^2 dr_\alpha\left\{\chi_\alpha^\theta(k,\ r_\alpha)\right\}^2.\qquad(2\cdot12)$$

The free continuum states $\Psi_{k_\theta^\alpha,0}^\theta$ are solutions for $H_0(\theta)$,

$$H_0(\theta)|\Psi_{k_\theta^\alpha,0}^\theta\rangle=E_{k_\theta^\alpha,0}|\Psi_{k_\theta^\alpha,0}^\theta\rangle\quad\text{and}\quad|\Psi_{k_\theta^\alpha,0}^\theta\rangle=\chi_{\alpha,0}^\theta(k_\theta^\alpha,\ r_\alpha)|\Phi_\alpha\rangle\rangle.\qquad(2\cdot13)$$

2.3. *Discretization of continuum*

As shown in the previous paper,[14)] the CSM enables us to calculate the second (resonance part) and third (continuum part) terms of Eq. (2·9) with the basis function method. In this method, the relative radial wavefunction of the channel α is approximately expressed with a finite number, N_α, of square-integrable (L^2) basis functions $\{\phi_n\}$,

$$\chi_\alpha^\theta(r)=\sum_{n=1}^{N_\alpha}c_n^\alpha(\theta)\phi_n(r),\qquad(2\cdot14)$$

where the channel suffix α of the radial coordinate r_α is left out, because only one radial coordinate exists in every channel of a two-body system. The energy eigenvalues in the continuum are rotated and discretized in the complex energy plane, as shown by black circles in Fig. 2. By the basis function expansion method, the CLD can be split into two parts

$$\Delta(E)\approx\rho_\theta^N(E)-\rho_{\theta(0)}^N(E).\qquad(2\cdot15)$$

In this approximation, Eq. (2·14), not only the bound and resonant states can be normalized but also the continuum eigenstates. When we integrate over every radial coordinate r in (2·10), we obtain

$$\rho_\theta^N(E)=-\frac{1}{\pi}\text{Im}\left[\sum_B^{N_B}\frac{1}{E-E_B}+\sum_R^{N_R^\theta}\frac{1}{E-E_R}+\sum_{k\in\text{C}}^{N-N_R^\theta-N_B}\frac{1}{E-\mathcal{E}_k(\theta)}\right].\qquad(2\cdot16)$$

The bound state contribution can be easily derived from the well-known expression $\frac{1}{E+i0-E_B}=\frac{P}{E-E_B}-i\pi\delta(E-E_B)$. In the calculation of the resonant and continuum contributions, the limit procedure, expressed by $+i0$, has no effect because E is a

real number while E_R and $\mathcal{E}_k(\theta)$ are complex numbers located in the lower half plane. Here, $\mathcal{E}_k(\theta)$ stands for a discretized continuum energy $E_{k_\theta^\alpha}$; $\alpha = 1 \ldots, n$.

As shown in Fig. 2, the contribution of each continuum eigenstate to the level density can be derived from eigenvalues, $\mathcal{E}_k(\theta) = \mathcal{E}_k^R - i\mathcal{E}_k^I$, of $H(\theta)$ in terms of a Lorentzian function,

$$\text{Im} \frac{1}{E - \mathcal{E}_k(\theta)} = \frac{-\mathcal{E}_k^I}{(E - \mathcal{E}_k^R)^2 + \mathcal{E}_k^{I2}}. \qquad (2\cdot17)$$

The continuum contribution is automatically smoothed out when we use a sufficiently large number of basis functions $\{\phi_n\}$ for a given scaling parameter θ. In the usual basis function method, a smoothing technique such as the Strutinsky procedure[15] is required to calculate the CLD,[2),3)] because the continuum is discretized on the real axis, and each continuum contribution has a delta-function form. As mentioned above, the present discretization method in the CSM creates no need for an auxiliary technique like the Strutinsky procedure; no singularity like the delta-function appears.

Finally, the level density can be calculated as

$$\rho_\theta^N(E) = \sum_B^{N_B} \delta(E - E_B)$$

$$+ \frac{1}{\pi} \sum_R^{N_R^\theta} \frac{\Gamma_r/2}{(E - E_r)^2 + \Gamma_r^2/4}$$

$$+ \frac{1}{\pi} \sum_{k \in C}^{N - N_R^\theta - N_B} \frac{\mathcal{E}_k^I}{(E - \mathcal{E}_k^R)^2 + \mathcal{E}_k^{I2}}, \qquad (2\cdot18)$$

where E_r and Γ_r are the energy and width of a resonant state, respectively. In the CSM, the eigenvalue of the resonance is expressed as $E_R = E_r - i\Gamma_r/2$, and then the resonance part has exactly the Breit-Wigner form.

As discussed in the previous paper,[14)] this expression of the level density is dependent on the scaling parameter θ, but this θ dependence disappears in the form of the CLD, $\Delta^N(E)$, which is defined as

$$\Delta^N(E) = \rho_\theta^N(E) - \rho_{\theta(0)}^N(E), \qquad (2\cdot19)$$

where $\rho_{\theta(0)}^N(E)$ is expressed in terms of the eigenvalues of the asymptotic Hamiltonian
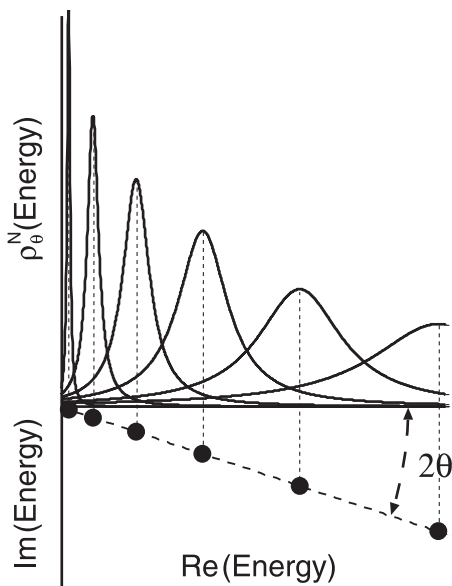

Fig. 2. Schematic energy eigenvalue distribution (black circles) for a complex scaled Hamiltonian and contributions to the level density (solid lines).

$H_0(\theta)$ as

$$\rho_{\theta(0)}^N(E) = -\frac{1}{\pi}\text{Im}\left[\sum_i^N \frac{1}{E - \mathcal{E}_i^0(\theta)}\right] \tag{2.20}$$

which has only continuum spectra. This result indicates a cancellation of the θ-dependences in $\rho_\theta^N(E)$ and $\rho_{\theta(0)}^N(E)$.

In the previous paper, it was also shown that $\Delta^N(E)$ gives a good description for $\Delta(E)$, which is the derivative of the phase shift for single-channel systems. For a generalization, the CLD is obtained as the right-hand side of Eq. (1.2) and represented as the sum of the derivatives of the eigenphases $\delta_j(E)$,[4]

$$\Delta(E) = \frac{1}{\pi}\sum_j \frac{d\delta_j}{dE}. \tag{2.21}$$

§3. Application

3.1. *Application to a 3N-N coupled-channel model*

We apply the present formalism to the $^4\text{He} = [^3\text{H}+p] + [^3\text{He}+n]$ cluster-model calculation.[23] In this model, the total wavefunction is expressed as

$$|\Psi^q(^4\text{He})\rangle = \chi_{^3\text{H}+p}^q(r)|\Phi_{^3\text{H}+p}^q\rangle\rangle + \chi_{^3\text{He}+n}^q(r)|\Phi_{^3\text{He}+n}^q\rangle\rangle, \tag{3.1}$$

where $\chi_{^3\text{H}+p}^q(r)$ and $\chi_{^3\text{He}+n}^q(r)$ are the relative radial wavefunctions of $^3\text{H}+p$ and $^3\text{He}+n$ channels, respectively, and q is an abbreviation of the quantum numbers $(^{2S+1}L_J)$. The channel wavefunctions of $^3\text{H}+p$ and $^3\text{He}+n$ systems are denoted as $\Phi_{^3\text{H}+p}^q$ and $\Phi_{^3\text{He}+n}^q$, respectively.

The relative radial wavefunctions $\chi_{^3\text{H}+p}^q(r)$ and $\chi_{^3\text{He}+n}^q(r)$ are obtained by solving the Schrödinger equation

$$H\,|\Psi^q(^4\text{He})\rangle = E\,|\Psi^q(^4\text{He})\rangle, \qquad H = T + V, \tag{3.2}$$

where T is the kinetic energy and V is the nuclear plus Coulomb potential.

The coupled-channel equations to be solved are given as

$$\left[-\frac{\hbar^2}{2\mu_{^3\text{H}+p}}\nabla^2 + V_D^q(r) + \frac{e^2}{r}\text{erf}(\sqrt{\beta}r) - E + \epsilon_{^3\text{H}+p}\right]\chi_{^3\text{H}+p}^q(r) = V_C^q(r)\chi_{^3\text{He}+n}^q(r),$$

$$\tag{3.3a}$$

$$\left[-\frac{\hbar^2}{2\mu_{^3\text{He}+n}}\nabla^2 + V_D^q(r) - E + \epsilon_{^3\text{He}+n}\right]\chi_{^3\text{He}+n}^q(r) = V_C^q(r)\chi_{^3\text{H}+p}^q(r), \tag{3.3b}$$

where β, in the Coulomb folding interaction, is taken to be 0.66 fm^2 from the observed r.m.s. radius of ^3He.

We also use the experimental threshold energy difference between $^3\text{He}+n$ and $^3\text{H}+p$ channels as

$$\epsilon_{^3\text{He}+n} - \epsilon_{^3\text{H}+p} = 0.763 \text{ MeV}, \tag{3.4}$$

and we set $\epsilon_{^3\mathrm{H}+p}$ as the origin of the complex energy plane.

The diagonal potential (V_D^q) and the coupling potential (V_C^q) are constructed from $T = 1$ and $T = 0$ components as

$$V_D^q(r) = \frac{1}{2}\left\{ V^{q,T=1} \exp\left[-\left(\frac{r}{b_{q,T=1}}\right)^2\right] + V^{q,T=0} \exp\left[-\left(\frac{r}{b_{q,T=0}}\right)^2\right] \right\} \quad (3\cdot5)$$

and

$$V_C^q(r) = \frac{1}{2}\left\{ V^{q,T=1} \exp\left[-\left(\frac{r}{b_{q,T=1}}\right)^2\right] - V^{q,T=0} \exp\left[-\left(\frac{r}{b_{q,T=0}}\right)^2\right] \right\}, \quad (3\cdot6)$$

where the parameters of the Gaussian forms are determined from the phase shift data of $^3\mathrm{H} + n$, $^3\mathrm{He} + n$, $^3\mathrm{H} + p$ and $^3\mathrm{He} + p$. The details of these potentials and the parameters used here are found in Refs. 23) and 24). For the $^3P_1$ state, $V^{q,T=1} = -18.83$ MeV, $V^{q,T=0} = -8.0$ MeV, $b_{q,T=1} = 3.06$ fm, $b_{q,T=0} = 3.0$ fm are obtained to reproduce the experimental phase shifts.

We employ the Gaussian basis functions[25] to describe the relative radial wavefunction, and the same parameters as those used in Ref. 14) are adopted for each channel. In this calculation, we use 30 Gaussian basis functions for every channel; hence, the total basis number is $N = 60$.

At first, we show the energy eigenvalue distributions of $^3P_1$ states in Fig. 3. With $\theta = 20°$ and $30°$ (left-hand side of Fig. 3), a resonance is not extracted and only continua appear. When we take $\theta = 40°$ (right-hand side of Fig. 3), the broad resonance $E_R = 1.89 - i2.46$ MeV is obtained. The continuum solutions deviate slightly from the 2θ-line, and the deviation increases for $\theta = 40°$. As shown in the
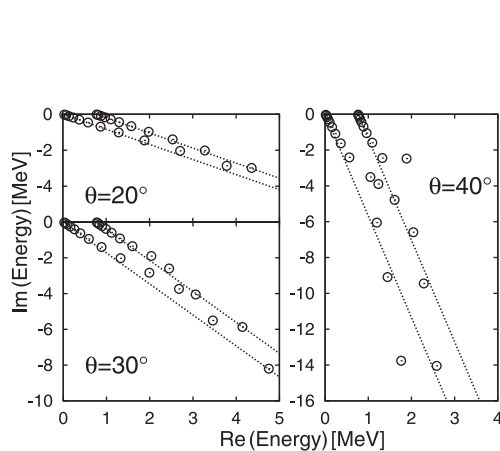

Fig. 3. Energy eigenvalues of the $^3P_1$ state with $\theta = 20°$ (left top), $\theta = 30°$ (left bottom) and $\theta = 40°$ (right). The circles represent energy eigenvalues and dotted lines are 2θ- lines.

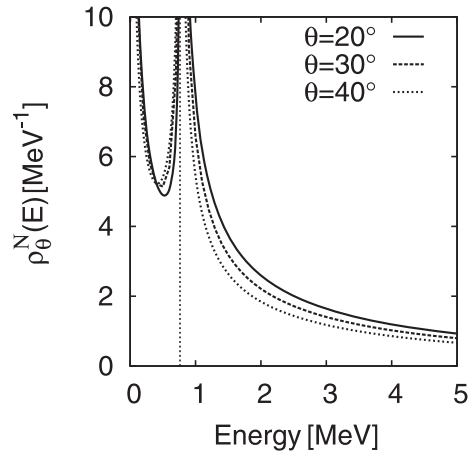Fig. 4. θ-dependence of calculated level densities $\rho_\theta^N(E)$ of the $^3P_1$ state. The vertical line indicates the threshold energy of the $^3\mathrm{He}+n$ system. In this calculation, $N = 60$ eigenvalues are used.
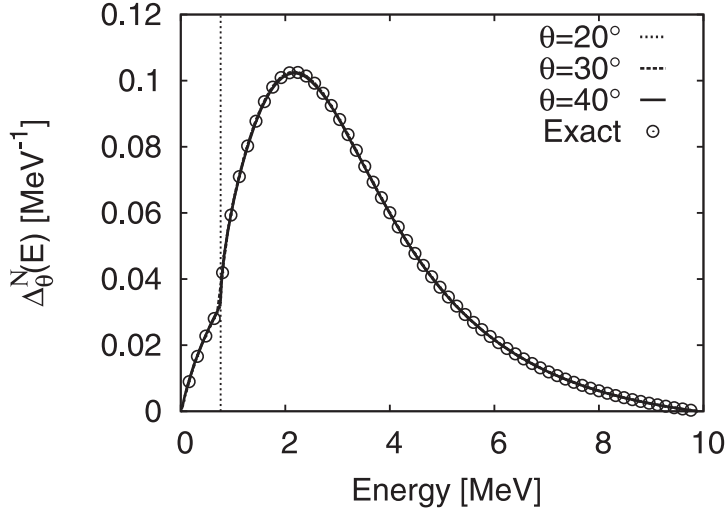
Fig. 5. Calculated CLD of $^3P_1$ state. The vertical dotted line indicates the threshold energy of the ^{3}He $+ n$ system.

previous paper and will be shown later, this energy deviation from the 2θ-line has no serious effect on the CLD calculations.

In Fig. 4, the calculated level density $\rho_\theta^N(E)$ of this system is shown. There are two peaks associated with the threshold. Similarly to the single-channel case, the quantity $\rho_\theta^N(E)$ has a θ-dependence and these peaks disappear if we calculate $\Delta^N(E)$ by subtracting $\rho_{0(\theta)}^N(E)$ from $\rho_\theta^N(E)$, which is obtained from eigenvalues of the asymptotic Hamiltonian with the Coulomb potential between ^{3}He and p:

$$\begin{pmatrix} -\frac{\hbar^2}{2\mu_{3\mathrm{H}+p}}\nabla^2 + e^2/r + \epsilon_{3\mathrm{H}+p}, & 0 \\ 0 & -\frac{\hbar^2}{2\mu_{3\mathrm{He}+n}}\nabla^2 + \epsilon_{3\mathrm{He}+n} \end{pmatrix}. \quad (3\cdot7)$$

The calculated CLD, $\Delta^N(E)$, is shown in Fig. 5. The "exact" dots represent the results obtained from the S-matrix form (Eq. (2·21)) which is calculated by solving Eqs. (3·3a) and (3·3b) with the Runge-Kutta method.

In Fig. 5, we can see that the calculated CLD $\Delta_\theta^N(E)$ in the CSM does not depend on the scaling parameter θ. The results with $\theta = 20°$, $30°$ and $\theta = 40°$ overlap each other. Therefore, we cannot distinguish the results obtained for different θ-values in Fig. 5. Two peaks associated with the thresholds shown in $\rho_\theta^N(E)$ disappear in the CLD. Instead, one broad peak associated with the resonance appears in $\Delta_\theta^N(E)$.

Moreover, we can see a good agreement with the "exact" calculation obtained from the S-matrix by solving the coupled-channel equations. From such results, we can confirm the good applicability of this formalism to coupled-channel systems.

The calculated resonance peak does not depend on whether the resonance energy is obtained as an isolated eigenvalue or not. With $\theta = 40°$, the ECR used in the CLD calculation is constructed from the resonance and continuum. As shown in Eq.

(2·18), the resonance part has the Breit-Wigner form and the continua describe the background contribution. On the other hand, with a small θ ($\theta = 20°$ or $\theta = 30°$), no resonance eigenvalue is obtained, but the resonance structure is reproduced in the CLD. In the calculations with a small θ, the ECR is constructed only from continuum states, and these rotated continuum states describe both the resonance peak around $E = 2$ MeV and the background contributions.

3.2. *Orthogonality condition model*

In this subsection, we study another numerical example. In the model for $^3\text{H}+p$ and $^3\text{He} + n$, where a $(0s_{1/2})^3$ configuration is assumed for ^3H and ^3He clusters, the S-wave relative motion between projectile and target for such systems has three Pauli-forbidden states (PFS) with zero node. The $^3S_1$ partial waves with $T = 0$ and $T = 1$ and one $^1S_0$ partial wave with $T = 1$ are the PFS. Other S states orthogonal to these PFS are Pauli-allowed states. We take into account the Pauli principle by employing the orthogonality condition model (OCM).[26] In this section, we calculate the CLD $\Delta_\theta^N(E)$ for the $^1S_0$ partial wave. The PFS is constructed using the harmonic oscillator wavefunction, $u_{n,l}(r)$ with $n = 0, l = 0$ as

$$\Psi_{PF}^{T=1}(^1S_0) = \frac{1}{\sqrt{2}}\left[u_{0,0}^{^3\text{H}+p}(r)\Phi_{^3\text{H}+p}(^1S_0) + u_{0,0}^{^3\text{He}+n}(r)\Phi_{^3\text{He}+n}(^1S_0)\right]. \quad (3\cdot8)$$

We add the following Pauli potential[27] into the Hamiltonian of Eq. (3·2);

$$V_{\text{Pauli}} = \lambda|\Psi_{PF}^{T=1}(^1S_0)\rangle\langle\Psi_{PF}^{T=1}(^1S_0)| \quad (3\cdot9)$$

to push the PFS into an unphysical energy region by taking a large positive value for λ. In the present calculation, λ is taken to be 10^6 MeV. We use the harmonic oscillator width $b_m = 1.61$ fm from the observed matter radius of ^4He. Finally, the coupled-channel equations for $^1S_0$ partial waves are rewritten from Eqs. (3·3a) and (3·3b) as

$$\left[-\frac{\hbar^2}{2\mu_{^3\text{H}+p}}\nabla^2 + V_D^q(r) + \frac{e^2}{r}\text{erf}(\sqrt{\beta}r) + \frac{\lambda}{2}|u_{0,0}^{^3\text{H}+p}(r)\rangle\langle u_{0,0}^{^3\text{H}+p}(r)| - E + \epsilon_{^3\text{H}+p}\right]\chi_{^3\text{H}+p}^q(r)$$

$$= \left[V_C^q(r) + \frac{\lambda}{2}|u_{0,0}^{^3\text{H}+n}(r)\rangle\langle u_{0,0}^{^3\text{He}+n}(r)|\right]\chi_{^3\text{He}+n}^q(r), \quad (3\cdot10a)$$

$$\left[-\frac{\hbar^2}{2\mu_{^3\text{He}+n}}\nabla^2 + V_D^q(r) + \frac{\lambda}{2}|u_{0,0}^{^3\text{He}+n}(r)\rangle\langle u_{0,0}^{^3\text{He}+n}(r)| - E + \epsilon_{^3\text{He}+n}\right]\chi_{^3\text{He}+n}^q(r)$$

$$= \left[V_C^q(r) + \frac{\lambda}{2}|u_{0,0}^{^3\text{He}+p}(r)\rangle\langle u_{0,0}^{^3\text{H}+p}(r)|\right]\chi_{^3\text{H}+p}^q(r). \quad (3\cdot10b)$$

The asymptotic Hamiltonian is not changed from Eq. (3·7), because the Pauli potential has a short range and no effect in the asymptotic region.

In this treatment, the potential parameters are obtained as $V^{q,T=1} = -7.55$ MeV, $V^{q,T=0} = -58.5$ MeV, $b_{q,T=1} = 3.0$ fm, and $b_{q,T=0} = 3.0$ fm for the $^1S_0$ state.

The calculated energy eigenvalue distribution is shown in Fig. 6 and the CLD is shown in Fig. 7. Here, we use $\theta = 35°$. In Fig. 6, no resonance is obtained. However,

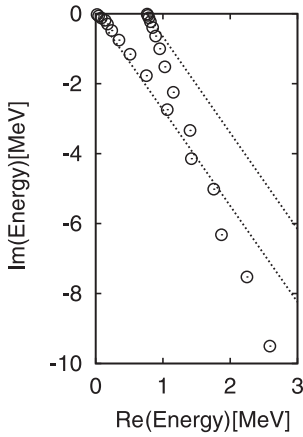Fig. 6. Energy eigenvalues (open circles) of $^1S_0$ state with $\theta = 35°$. The dotted lines are the 2θ-lines.
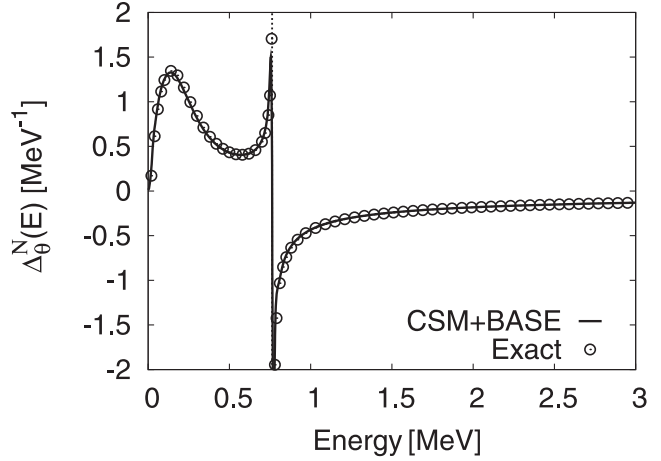
Fig. 7. Calculated CLD of $^1S_0$ state. The vertical dotted line is the threshold of the $^3\mathrm{He} + n$ system.

in the CLD, there is one peak at low energy and we can see the cusp at the threshold energy.

We compare the result obtained using the present formalism with the "exact" calculation of the CLD from the S-matrix. In the present calculation of the S-matrix, we solve the coupled-channel equation using the Jost function method (JFM)[28] with the OCM[29] for treating the nonlocal potential term. We can see that the present formalism works well even if the potential contains a nonlocal part with very large coefficients (10^6) indicating an almost singular behavior.

Using the JFM-OCM,[29] the S-matrix pole is obtained at $E_R = 0.14 - i0.21$ MeV. We can then understand that the peak of CLD at low energy is caused by the resonance. In the usual CSM with a finite number of basis functions, it is difficult to obtain such a resonance with such a large width $\Gamma/2 > E_r$, since, as shown in Fig. 6, the resonance is not clearly separated from the continua. To investigate this kind of resonance, it is necessary to use an additional method such as the analytical continuation of a coupling constant (ACCC)[30] together with the complex scaling method.[31],[32]

The CLD in the CSM has a great advantage: we can obtain the resonance peak even if the resonance is not isolated by the CSM.

§4. Definition of density in a coupled-channel system

In this section, we discuss the matrix form of the CLD. In coupled-channel systems, a Green's function is expressed as the following matrix form,

$$\langle r|G(E)|r'\rangle = \begin{pmatrix} G_{11}(r,r') & G_{12}(r,r') & \cdots \\ G_{21}(r,r') & G_{22}(r,r') & \cdots \\ \vdots & \vdots & \ddots \end{pmatrix}, \qquad (4\cdot1)$$

and we also define an operator matrix $\mathbf{\Gamma}$ as

$$\mathbf{\Gamma}(r,r') \equiv \langle r|G(E) - G_0(E)|r'\rangle = \begin{pmatrix} \Gamma_{11}(r,r') & \Gamma_{12}(r,r') & \cdots \\ \Gamma_{21}(r,r') & \Gamma_{22}(r,r') & \cdots \\ \vdots & \vdots & \ddots \end{pmatrix}, \quad (4\cdot2)$$

where $G - G_0$ results from $V = H - H_0$ as

$$G - G_0 = GVG_0 = G_0VG. \quad (4\cdot3)$$

Therefore, Eq. (1·2) becomes

$$\Delta(E) = -\frac{1}{\pi}\mathrm{Im}\int r^2 dr\,\{\Gamma_{11}(r,r) + \Gamma_{22}(r,r) + \cdots\}. \quad (4\cdot4)$$

Consider the term, $-\frac{1}{\pi}\mathrm{Im}\int r^2 dr\,\Gamma_{\alpha\alpha}$, as a density in channel α. Diagonalizing the matrix $\mathbf{\Gamma}(r,r)$, we obtain

$$\begin{pmatrix} \lambda_{11}(r,r) & 0 & 0 \\ 0 & \lambda_{22}(r,r) & 0 \\ 0 & 0 & \ddots \end{pmatrix}. \quad (4\cdot5)$$

Therefore, the total level density is represented as

$$\Delta(E) = -\frac{1}{\pi}\mathrm{Im}\int r^2 dr\,\{\lambda_{11}(r,r) + \lambda_{22}(r,r) + \cdots\}, \quad (4\cdot6)$$

and the partial density in the "eigenchannel" c is expressed as $-\frac{1}{\pi}\mathrm{Im}\int r^2 dr\,\lambda_{cc}$.

Applying the CSM with the basis function method, we calculate the matrix elements of $\mathbf{\Gamma}$

$$\begin{aligned} \Gamma^N_{\alpha,\beta}(r,r') &= \langle\langle\Phi_\alpha|\left\langle r\left|\left[\frac{1}{E-H} - \frac{1}{E-H_0}\right]\right|r'\right\rangle|\Phi_\beta\rangle\rangle \\ &= \sum_{k=1}^{N}\left[\frac{\chi^\theta_{\alpha,k}(r)\chi^\theta_{\beta,k}(r')}{E - E^\theta_k} - \frac{\chi^{\theta,(0)}_{\alpha,k}(r)\chi^{\theta,(0)}_{\beta,k}(r')}{E - E^\theta_{k(0)}}\right]. \end{aligned} \quad (4\cdot7)$$

From this expression of the $\mathbf{\Gamma}$ matrix elements, we obtain CLD matrix elements between channels α and β as

$$\Delta^N_{\alpha,\beta}(E) = -\frac{1}{\pi}\mathrm{Im}\int r^2 dr\,\Gamma^N_{\alpha,\beta}(r,r). \quad (4\cdot8)$$

By diagonalizing this $\Delta^N_{\alpha,\beta}$, we can define the CLD in the so called eigenchannels of the coupled-channel system.

We calculate these quantities for the $[^3\mathrm{H}+p]+[^3\mathrm{He}+n]$ coupled-channel system with the CSM. Results for the $^1P_1$ state are shown in Fig. 8. It provides results calculated with $\theta = 20°$ and $40°$ and $N = 60$. Channel labels 1 and 2 denote $^3\mathrm{H}+p$ and $^3\mathrm{He}+n$, respectively. From such results, we can see that there is no θ dependence
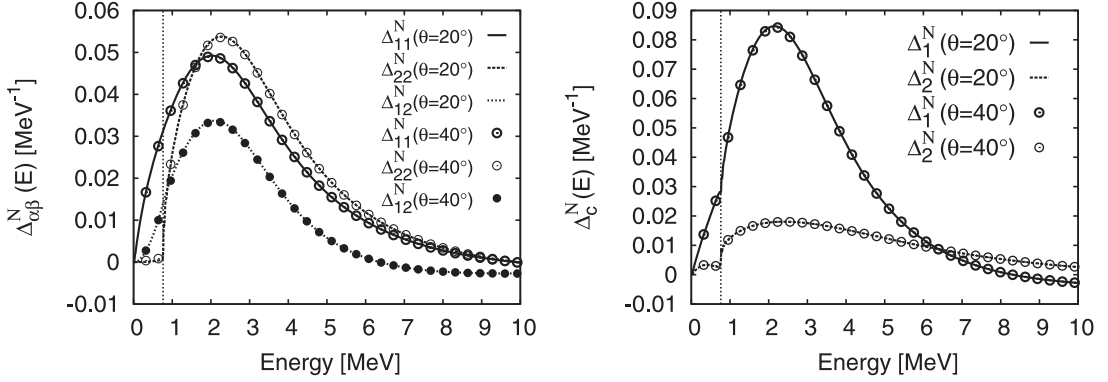
Fig. 8. Calculated coupled-channel CLDs $\Delta_{\alpha,\beta}^N(E)$ of $^1P_1$ states. The left-hand side shows the matrix form of the CLD and the right-hand side shows the CLD in the eigenchannels. The calculated results with $\theta = 20°$ and $40°$ are presented in lines and circles, respectively, where $N = 60$. The channels 1 and 2 denote ^{3}H+p and ^{3}He+n, respectively. The vertical line is the threshold of the ^{3}He + n system.

in the matrix elements $\Delta_{\alpha,\beta}^N(E)$ and the eigenchannel partial CLDs $\Delta_c^N(E)$. In this energy region, both channels have the same contribution to the CLD. However, the eigenchannel CLDs show that eigenchannel 1 has the dominant contribution.

To see the physical meaning of eigenchannel partial CLDs, we calculated the phase shifts from $\Delta_c^N(E)$ and compared with the eigenphase shifts. In the single-channel case, the phase shift $\delta_l(E)$ is calculated as $\delta_l(E) = \int_0^E dE' \Delta(E')$. However, in the case of coupled-channel systems, the eigenphase shifts are not reproduced by a formula $\delta_c(E) = \int_0^E dE' \Delta_c(E')$ from the partial CLD of the eigenchannel, although the derivative of the eigenphase shifts sum is equivalent to the trace of the matrix $\Delta_{\alpha,\beta}^N(E)$ as shown in Fig. 5.

§5. Summary and conclusion

In this paper, we have formulated the CLD for coupled-channel systems. We have shown that the CLD with the CSM and the basis function method works well for coupled-channel systems. The CLD is also formulated in a matrix form where matrix elements enable us to investigate the contribution of each channel. Such results prove numerically that the ECR works also for coupled-channel systems.

Recently, it has also been shown that scattering amplitudes are obtained from complex scaling.[33] In the method, we can calculate the scattering amplitudes without an explicit enforcement of boundary conditions. However, the method demands the calculation of matrix elements between basis functions and regular asymptotic functions (Bessel or Coulomb functions). This task becomes harder in more complex systems.

The CLD formalism is very convenient because it does not demand further calculations. This method gives a great opportunity to investigate scattering properties, from those eigenvalues calculated for resonant states and bound states within an

L^2 basis set. Therefore, the CLD acts as a mediator between nuclear structure and scattering information.

Usually, to calculate with the CSM, a resonant state with a complex wave number $k_R = \kappa - i\gamma$, one must take θ such that $\gamma/\kappa < \tan\theta$. However, if the system is complex, it becomes difficult to take a large value of θ.[31),32)] In the CLD formalism, the complex scaling is mainly used to smooth the continuum contribution, and one can obtain, from the CLD with small θ values, information about resonances. There is no restriction for the θ value for an investigation of resonances in this formalism.

In coupled-channel systems with rearrangement, an interesting problem of shadow poles has been discussed for ^{5}He.[34)] This problem, unfortunately, is out of scope in the present CLD discussion. To investigate shadow poles, we have to solve the complex scaled Schrödinger equation with different scaling angles for every channel or within the multimomentum plane. This is left as a future work. Another future problem concerns the CLD in three-body systems.[35)] Recently, we have studied several types of three-body resonances in the 3α system. A calculation of the CLD of the 3α system is now in progress.

Acknowledgements

References

1) S. Shlomo, Nucl. Phys. A **539** (1992), 17.
2) A. T. Kruppa, Phys. Lett. B **431** (1998), 237.
3) A. T. Kruppa and K. Arai, Phys. Rev. A **59** (1999), 3556.
4) R. D. Levine, *Quantum Mechanics of Molecular Rate Processes* (Clarendon Press, Oxford, 1969), p. 101.
5) T. Y. Tsang and T. A. Osborn, Nucl. Phys. A **247** (1975), 43.
6) T. A. Osborn and T. Y. Tsang, Ann. of Phys. **101** (1976), 119.
7) S. Shlomo, V. M. Kolomietz and H. Dejbakhsh, Phys. Rev. C **55** (1997), 1972.
8) T. Vertse, A. T. Kruppa and W. Nazarewicz, Phys. Rev. C **61** (2000), 064317.
9) K. Arai and A. T. Kruppa, Phys. Rev. C **60** (1999), 064315.
10) J. Aguilar and J. M. Combes, Commun. Math. Phys. **22** (1971), 269.
    E. Balslev and J. M. Combes, Commun. Math. Phys. **22** (1971), 280.
11) Y. K. Ho, Phys. Rep. **99** (1983), 1.
12) N. Moiseyev, Phys. Rep. **302** (1998), 212.
13) S. Aoyama, T. Myo, K. Katō and K. Ikeda, Prog. Theor. Phys. **116** (2006), 1.
14) R. Suzuki, T. Myo and K. Katō, Prog. Theor. Phys. **113** (2005), 1273.
15) V. M. Strutinsky, Nucl. Phys. A **95** (1967), 420.
16) V. A. Mandelshtam, T. R. Ravuri and H. S. Taylor, Phys. Rev. Lett. **70** (1993), 1932.
17) V. A. Mandelshtam, H. S. Taylor, V. Ryaboy and N. Moiseyev, Phys. Rev. A **50** (1994), 2764.
18) T. Berggren, Nucl. Phys. A **109** (1968), 265.
19) T. Myo, A. Ohnishi and K. Katō, Prog. Theor. Phys. **99** (1998), 801.
20) B. G. Giraud and K. Katō, Ann. of Phys. **308** (2003), 115.
21) B. G. Giraud, K. Katō and A. Ohnishi, J. of Phys. A **37** (2004), 11575.
22) N. Moiseyev, P. R. Certain and F. Weinhold, Mol. Phys. **36** (1978), 1613.
23) M. Teshigawara, Doctor Thesis (1993, Hokkaido University).

24) M. Teshigawara, K. Katō and G. F. Filippov, Prog. Theor. Phys. **92** (1994), 79.
25) M. Kamimura, Phys. Rev. A **38** (1988), 621.
   H. Kameyama, M. Kamimura and Y. Fukushima, Phys. Rev. C **40** (1989), 974.
26) S. Saito, Prog. Theor. Phys. **41** (1969), 705.
27) V. M. Krasnopol'skiĭ and V. I. Kukulin, Sov. J. Nucl. Phys. **20** (1975), 470.
28) S. A. Sofianos and S. A. Rakityansky, J. of Phys. A **30** (1997), 3725; J. of Phys. A **31** (1998), 5149.
29) H. Masui, C. Kurokawa and K. Katō, Prog. Theor. Phys. **110** (2003), 233.
30) V. I. Kukulin and V. M. Krasnopol'sky, J. of Phys. A **10** (1977), L33.
   V. I. Kukulin, V. M. Krasnopol'sky and M. Miselkhi, Sov. J. Nucl. Phys. **29** (1979), 421.
31) S. Aoyama, Phys. Rev. C **68** (2003), 034313.
32) C. Kurokawa and K. Katō, Phys. Rev. C **71** (2005), 021301(R); Nucl. Phys. A **792** (2007), 87.
33) A. T. Kruppa, R. Suzuki and K. Katō, Phys. Rev. C **75** (2007), 044602.
34) A. Csótó, R. G. Lovas and A. T. Kruppa, Phys. Rev. Lett. **70** (1993), 1389.
35) J. P. Svenne, T. A. Osborn, G. Pisent and D. Eyre. Phys. Rev. C **40** (1989), 1136.